

Fractional Anisotropy Fiber Integration (FAFI) Improves Detection of Heterogeneous White Matter Alteration

Paolo GP Nucifora^{1*}, Jeffrey B Ware², Michael J Gawrysiak³, Elizabeth Whipple⁴, Ron L Wolf⁵, Rosette C Biester⁶, Richard J Ross⁷ and Keith M Robinson⁶

¹Departments of Radiology and Neurology, Loyola University Medical Center, Maywood, IL

²Department of Radiology, University of Pennsylvania, Philadelphia, PA

³Department of Psychology, Delaware State University, Dover, DE

⁴Department of Psychology, Drexel University, Philadelphia, PA

⁵Department of Radiology, University of Pennsylvania, Philadelphia, PA

⁶Department of Rehabilitation Medicine, Corporal Michael J. Crescenz VA Medical Center, Philadelphia, PA

⁷Department of Psychiatry, Corporal Michael J. Crescenz VA Medical Center, Philadelphia, PA

Received March 14, 2016; Accepted May 25, 2016; Published July 10, 2016

ABSTRACT

Objectives: Diffusion magnetic resonance imaging can provide a unique perspective into the structural properties of white matter in health and disease. Track-weighted techniques are a promising means of evaluating these images for white matter pathology, particularly when the burden of disease is distributed heterogeneously across white matter tracts. However, to our knowledge the accuracy of track-weighted techniques has not been tested in a ground truth environment.

Materials and Methods: We constructed ground truth datasets with simulated lesions that consistently involved either the corticospinal tract or the cingulum. The location of lesions within an affected tract varied for each individual. We also implemented a track-weighted metric designed to detect spatially heterogeneous white matter alterations in a variety of settings, "Fractional Anisotropy Fiber Integration" (FAFI). Using our ground truth datasets, voxelwise analysis of fractional anisotropy (FA) maps was compared to voxelwise analysis of FAFI maps.

Results: We report that voxelwise analysis of FAFI maps resulted in a successful depiction of simulated lesions of both the corticospinal tract and the cingulum. Unlike many voxelwise approaches, abnormal tracts were revealed in near-tractographic detail. Unlike directed tractography, this analysis did not require *a priori* hypotheses regarding lesion location. Furthermore, there were no falsely discovered white matter abnormalities. In contrast, voxelwise analysis of FA maps failed to demonstrate the simulated lesions. Tract-based spatial statistics of FA maps likewise did not demonstrate the simulated lesions.

Conclusion: Track-weighted techniques such as FAFI may be useful in the evaluation of diseases that are believed to manifest with spatially heterogeneous white matter abnormalities.

Keywords: Diffusion imaging, Tractography, White matter

INTRODUCTION

Diffusion magnetic resonance imaging uses the signal of water diffusion to probe the organization of white matter in vivo [1-3]. Microstructural elements in white matter present barriers to the movement of water, and their organizational integrity can be assessed by measuring the directional preference (anisotropy) of water diffusion. When modeling diffusion as a tensor, regions of the brain with potential white matter disruption commonly demonstrate abnormalities in fractional anisotropy (FA) or other diffusion metrics.

Corresponding author: Paolo GP Nucifora, Departments of Radiology and Neurology, Loyola University Medical Center, Maywood, IL, USA. Email: paolo.nucifora@lumc.edu

Citation: Nucifora P GP, Ware J B, Gawrysiak M J, Whipple E, Wolf R L, et al. (2016) Fractional Anisotropy Fiber Integration (FAFI) Improves Detection of Heterogeneous White Matter Alteration. J Neurosurg Imaging Techniques, 1(2) 98: 50

Copyright: ©2016 Nucifora P GP, Ware J B, Gawrysiak M J, Whipple E, Wolf R L, et al. This is an open-access article distributed under the terms of the Creative Commons Attribution License, which permits unrestricted use, distribution, and reproduction in any medium, provided the original author and source are credited.

Group comparisons of diffusion metrics generally rely on voxel-to-voxel or region-to-region comparisons of diffusion metrics. However, white matter tracts almost always span multiple voxels and often span multiple regions. Thus, a diseased tract could escape detection if there were sufficient individual variation in the location of affected voxels or regions. A new class of track-weighted metrics, proposed by Correia et al. [4] and further developed by several groups, could improve sensitivity for heterogeneously distributed tract pathology. These metrics include "track density imaging" (TDI) [5-7], "average path length map" (APM) [8,9], and others. They are based on whole-brain tractography, which depicts the connectivity of every white matter voxel to every other voxel. In a TDI map, the value of a voxel is based on the number of streamlines passing through it. In an APM map, the value of a voxel is based on the length of its streamlines to other voxels. Using these techniques, voxels may demonstrate abnormal values not only if they are affected by disease, but also if they are connected to a voxel affected by disease.

Abnormalities in either TDI values or APM values indicate that abnormal fiber track termination may have occurred during whole-brain tractography. Fiber track termination occurs when a threshold is exceeded, for example when a fiber track enters a region of low FA or makes a sharp turn [3]. Although low FA is normally found in cortex, it is also found in diseased white matter [2,3]. Thus, fiber track termination events are more frequent in disease states.

Track-weighted maps may provide more sensitive depictions of abnormal white matter than conventional diffusion metrics, such as FA maps. But to our knowledge, track-weighted maps have not previously been compared to FA maps or other metrics in a ground-truth environment, with full knowledge of the location of affected white matter. We have constructed a synthetic system that simulates widely scattered lesions to two white matter tracts, the corticospinal tract and the cingulum. We have also implemented a track-weighted metric, "Fractional Anisotropy Fiber Integration" (FAFI), that is sensitive to white matter changes even if they do not result in fiber track termination. In a FAFI map, each voxel is used as a seed for a tractography streamline. The FAFI value of the voxel is defined as the path integral of FA over that tractography streamline (S), as follows:

$$S(t) = (x, y, z)$$

$$FAFI = \int_S FA(x, y, z) dt$$

Like other diffusion metrics, FAFI maps can be compared directly using whole-brain techniques without need for *a priori* hypotheses regarding the location of an abnormality. In patients with traumatic brain injury, FAFI can demonstrate relationships to clinical outcomes that are not evident when examining FA maps [10]. In this paper, we

examine the hypothesis that whole-brain analysis of FAFI maps can identify simulated white matter lesions more readily than a similar analysis of FA maps.

METHODS

All study protocols were approved by the local institutional review board. Informed consent was not obtained because the data were analyzed anonymously from a public database.

The study sample was composed of 40 healthy volunteers (19 male, 21 female, age 22 to 35 years). All diffusion images were provided by the Human Connectome Project [11]. Isotropic diffusion images were acquired on a 3T scanner (Siemens Skyra) with the following sequence parameters: repetition time = 5520 msec, echo time = 89.5 msec, flip angle = 78, field of view = 210 x 180 cm, matrix = 168 x 144, slice thickness = 1.25. Three diffusion weighting shells were used with $b = 1000, 2000, \text{ and } 3000$ s/mm², each with approximately 90 diffusion weighting directions and six $b = 0$ acquisitions [12-15].

Maps of FA and the principal eigenvector were produced using all three b values in FSL [16,17]. The unaltered FA maps were used as controls. Tractography of the left corticospinal tract and left cingulum was performed for each subject using the FACT algorithm [18]. From the tractography results, simulated lesions in each tract were generated. Each control individual had two synthetic counterparts: one with a simulated lesion in the left corticospinal tract and one with a simulated lesion in the left cingulum. For each voxel within the simulated lesions, the FA values and principal eigenvector were replaced by the corresponding values from a different voxel chosen randomly from within the brain. This method was designed to produce spatial and inter individual variation in lesion appearance, mimicking natural variation in pathophysiology.

Simulated lesions in each tract were produced within a single cross-sectional slice of the tract. The remainder of the tract was not altered. In order to minimize lesion overlap between individuals, no two simulated lesions were placed on the same slice (based on the scanner reference frame). For the corticospinal tract, which lies approximately along the craniocaudal axis, simulated lesions were "cut" along different axial planes. For the cingulum, which lies approximately along the anteroposterior axis, simulated lesions were "cut" along different coronal planes. Apart from the presence of simulated lesions, the synthetic groups were identical to the original control group. Right-sided tracts were not manipulated, serving as internal controls.

FAFI maps were produced from the control dataset and both synthetic datasets using an in-house MATLAB (MathWorks) script, which takes only the FA maps and principal eigenvector maps as input. To determine the FAFI value of a voxel, its center was used as the origin of a bidirectional streamline using the Fiber Assignment by Continuous Tractography algorithm [18]. Streamlines were

terminated in regions with FA less than 0.18, after an angular deviation greater than 45 degrees, or after revisiting a voxel. The FAFI value was estimated as the sum of FA values along the streamline, sampled at 1 mm intervals. The process was repeated for every voxel, taking approximately 40 minutes of computing time per brain volume on a personal computer. The resolution of FAFI maps and FA maps were identical. Whole-brain tractography used in producing FAFI maps was performed independently of directed tractography used to produce simulated lesions.

FA and FAFI maps were brain extracted and aligned into a common space using a nonlinear registration tool [19-21]. Images were masked to white matter, defined as $FA > 0.3$. Voxelwise comparisons of the control group to the simulated lesion groups was carried out using a permutation analysis (5000 permutations) at a two-tailed significance threshold of $p < 0.05$.

For FA maps only, statistical analysis was repeated using TBSS (Tract-Based Spatial Statistics, [22]), part of FSL [17]. This included additional preprocessing steps in which the mean FA map was generated and thinned to create a mean FA skeleton that represented the centers of all tracts common to the group. Each subject's aligned FA data was then projected onto this skeleton and masked to the skeleton before undergoing permutation analysis as above.

RESULTS

Simulated lesions were fairly small, with mean lesion volume of $147 \text{ mm}^3 \pm 27 \text{ mm}^3$ in the simulated corticospinal lesion group and mean lesion volume of $53 \text{ mm}^3 \pm 12 \text{ mm}^3$ in the simulated cingulum lesion group. As expected, FAFI maps depicted visible changes in lesion voxels as well as in voxels with normal FA that were in the affected white matter tract (**Figure 1**).

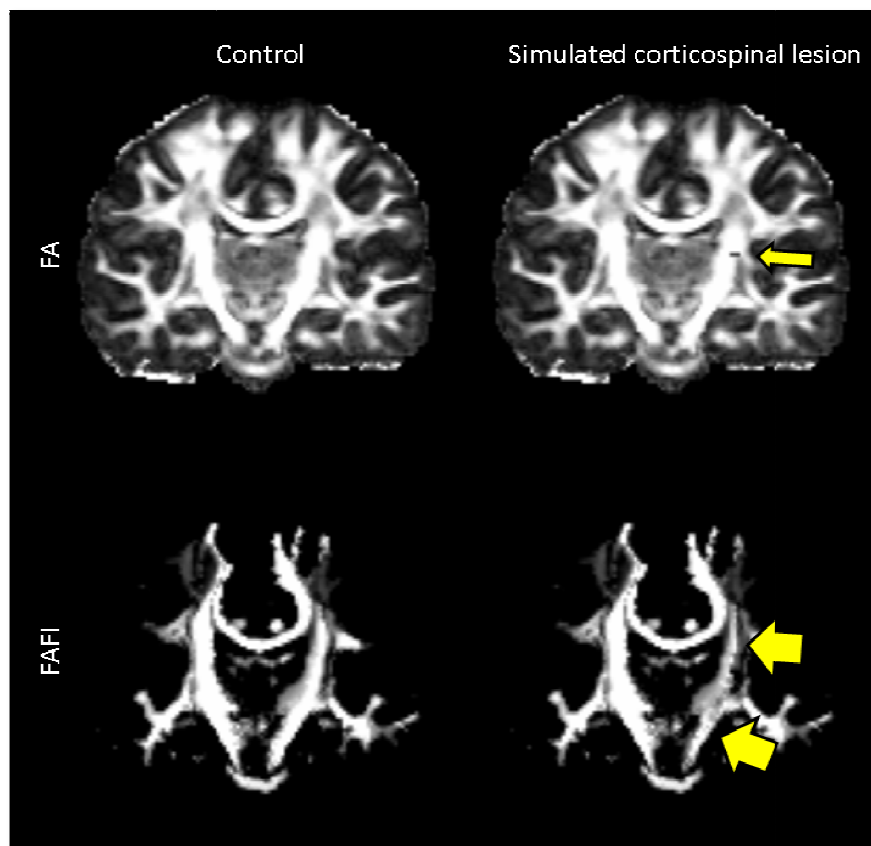


Figure 1. Coronal FA maps (top) and FAFI maps (bottom) from one representative subject.

Because they reflect macrostructure as well as microstructure, FAFI maps tended to produce greater contrast for highly-connected white matter.

Control images with unaltered white matter (left) were compared to their counterparts with a simulated lesion in the corticospinal tract (right). The location of the simulated lesion is indicated with a small yellow arrow. The simulated lesion caused visible asymmetric decreases in FAFI values throughout the corticospinal tract, even in white matter with normal FA values (large yellow arrows).

Voxelwise comparison of the control group to the simulated corticospinal lesion group demonstrated significantly decreased FAFI values in nearly every voxel of the main body of the corticospinal tract (**Figure 2**). Similarly, voxelwise comparison of the control group to the simulated cingulum lesion group demonstrated significantly decreased

FAFI values in nearly every voxel of the main body of the cingulum (**Figure 3**). When voxels with abnormal FAFI values were rendered in three dimensions, the affected tract was revealed in sufficient detail to identify it based on its gross anatomy. There was no need for post-hoc tractography.

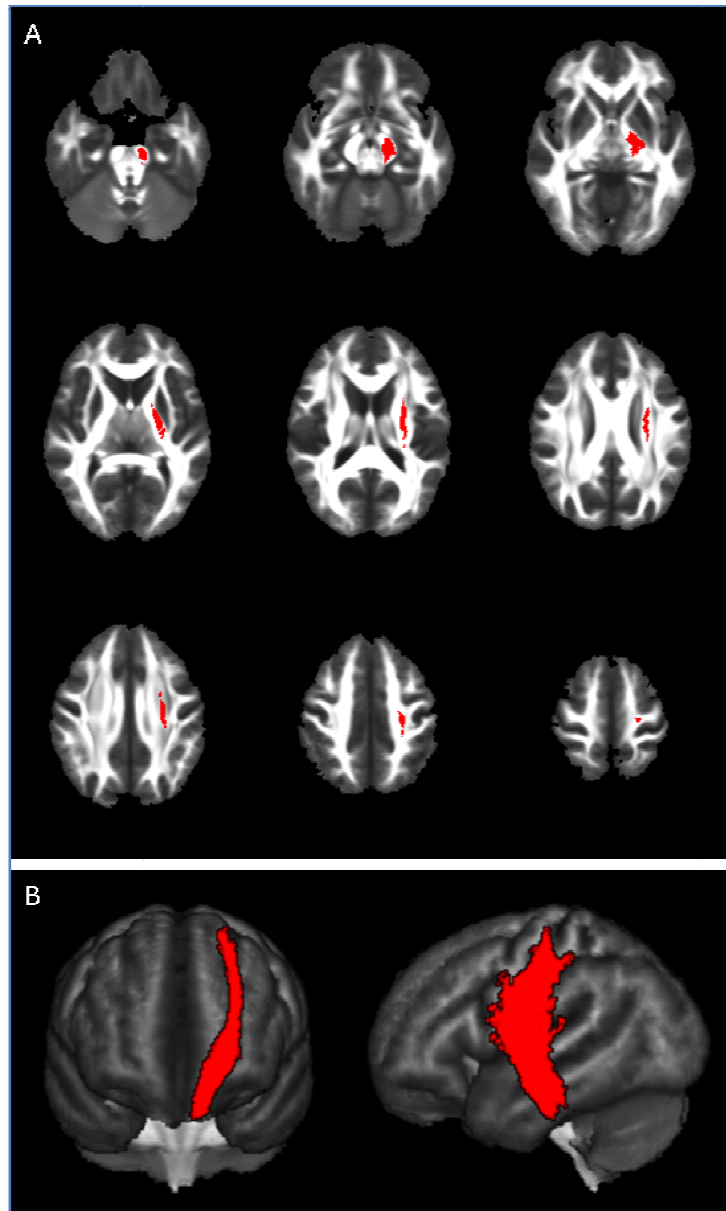


Figure 2. Voxelwise comparison of control group to simulated corticospinal lesion group.

(A) Decreased FAFI values were present throughout the expected location of the left corticospinal tract, depicted as an overlay ($p < 0.05$, red) on axial FA maps. (B) The left corticospinal tract was clearly identified after frontal and lateral 3D rendering of voxels with decreased FAFI values ($p < 0.05$, depicted in red), without the need for additional user-directed tractography.

No significant differences in FA values were observed using voxelwise comparisons with or without TBSS ($p < 0.05$).

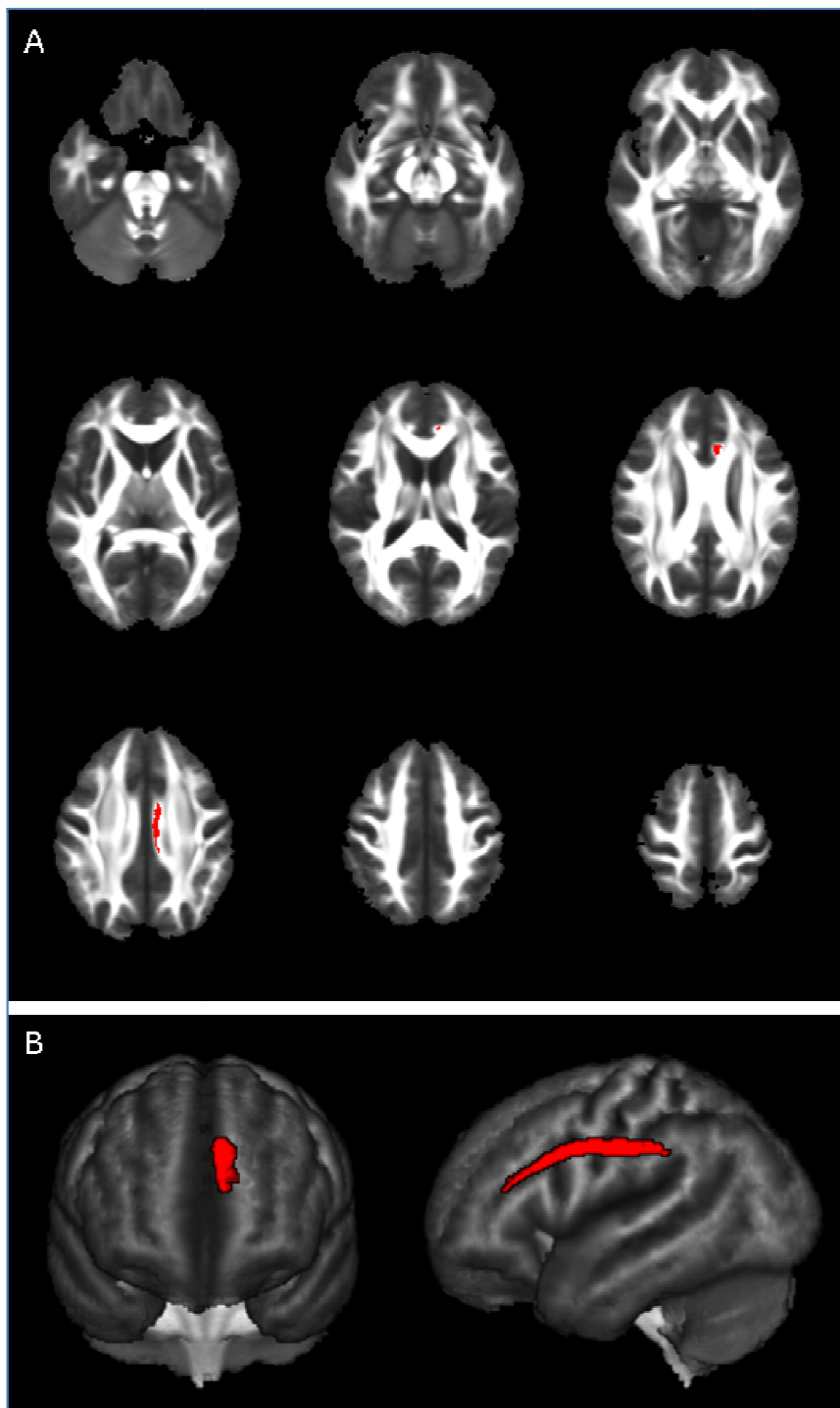


Figure 3. Voxelwise comparison of control group to simulated cingulum lesion group.

(A) Decreased FAFI values were present throughout the expected location of the left cingulum, depicted as an overlay ($p < 0.05$, red) on axial FA maps. (B) The left cingulum was clearly identified after frontal and lateral 3D rendering of voxels with decreased FAFI values ($p < 0.05$, depicted in red), without the need for additional user-directed tractography.

No significant differences in FA values were observed using voxelwise comparisons with or without TBSS ($p < 0.05$).

In both simulated lesion groups, no voxels demonstrated increased FAFI values. Decreased FAFI values were found exclusively in the left cerebral hemisphere (i.e. there were no falsely discovered voxels in the right hemisphere).

A parallel analysis using only FA maps found no voxels with significant FA differences between the control group and either of the simulated lesion groups. When the FA-only analysis was repeated using tract-based spatial statistics, we again found no voxels with significant FA differences between the control group and either of the simulated lesion groups.

DISCUSSION

Several diseases, including traumatic brain injury [23-25] and multiple sclerosis [26], manifest with an unpredictable multifocal pattern of abnormal white matter. In other diseases, such as schizophrenia [27], there is evidence of white matter involvement without a consensus on which white matter tracts, if any, are specifically involved. The simulated lesions described here are intended as a general model of diseases which consistently involve specific white matter tracts but do not consistently involve the same location of the tracts. We report the successful implementation of a method to detect spatially heterogeneous white matter alterations, and we demonstrate its advantages compared to a similar analysis of FA maps.

Directed tractography and other techniques have also been used to probe specific white matter tracts in health and diseases [16, 28-31]. However, directed tractography can be performed only when there are one or more tracts that are suspected to be abnormal. In contrast to directed tractography, FAFI maps can identify abnormal tracts even without *a priori* suspicion. In this study, alterations in the corticospinal tract and cingulum were identified based solely on an unbiased whole-brain analysis.

FAFI maps may be especially useful in disease states involving white matter tracts that are anatomically novel or grossly distorted. Furthermore, FAFI and FA maps may be used in a complementary manner when investigating a disease population. When FA comparisons are similar to FAFI comparisons, lesions most likely occur in consistent locations across the population. When there is mismatch, lesions most likely occur in different locations for each individual. For this reason, population-based standard atlases may prove as helpful for FAFI as they are for FA.

The method used to produce simulated lesions in this paper, which does not directly mimic any disease process, naturally limits its applicability to clinical settings. Although this method is arbitrary, we have found that similar results can be obtained by simply reducing FA [32]. In addition, only one tract was manipulated in each individual in order to highlight the ease of identifying the affected tracts. In a clinical setting, FAFI may demonstrate abnormalities in multiple

white matter tracts [10]. Consequently, identifying individual tracts via post-hoc inspection of FAFI results might be more challenging. Even in this case, we expect FAFI to offer advantages over FA analysis. One would still not require a priori knowledge of the affected white matter, nor would detection depend on consistency in lesion location within a tract.

A limitation common to FAFI and other track-weighted maps is the lack of a clear histological correlate for abnormal values. A voxel with decreased FA values is generally considered to reflect a focal microstructural abnormality of the underlying white matter [33]. A voxel with decreased FAFI values may likewise reflect a focal microstructural abnormality, but other explanations include reorientation or disorganization of white matter some distance away. FAFI values are sensitive to microstructural as well as macrostructural abnormalities, and therefore FAFI maps are a less specific indicator of pathology.

As with any technique that makes use of tractography, it should be noted that streamlines produced by fiber tracking are only a mathematical model of diffusion, which is not necessarily equivalent to physical white matter fibers [34]. Particularly when using derivatives of diffusion metrics such as FAFI, it is possible that abnormal values reflect pathophysiology in water movement that is unrelated to white matter injury. Furthermore, any method based on tractography may be more sensitive to tracking errors (particularly in regions of crossing and/or “kissing” fibers) than one based solely on FA. Other models (e.g. probabilistic tractography) may be more robust to tracking errors [35], but they are not easily applied to FAFI because probability estimates do not readily translate into fiber trajectories along which one can integrate FA.

In summary, we have presented a model for white matter injury that acknowledges potential spatial heterogeneity, illustrated with a ground-truth example of simulated lesions. We have introduced FAFI, a method to detect this sort of injury, and applied it to simulated lesions. Finally, we have explored the output of our FAFI analysis and compared it to the output of FA analysis. We believe that this method may be useful in the assessment of neuropathology, particularly when no well-defined locus is apparent with other DTI metrics.

ACKNOWLEDGMENTS

Data were provided by the Human Connectome Project, WU-Minn Consortium (Principal Investigators: David Van Essen and Kamil Ugurbil; 1U54MH091657) funded by the 16 NIH Institutes and Centers that support the NIH Blueprint for Neuroscience Research; and by the McDonnell Center for Systems Neuroscience at Washington University.

REFERENCES

1. Bihan DL, Breton E, Lallemand D, Grenier P, Cabanis E, and M. Laval-Jeantet, et al. (1986) MR imaging of intravoxel incoherent motions: application to diffusion and perfusion in neurologic disorders. *Radiology* 161: 401-407.
2. Basser PJ (1995) Inferring microstructural features and the physiological state of tissues from diffusion-weighted images. *NMR Biomed* 8: 333-344.
3. Nucifora PGP, Verma R, Lee SK, Melhem ER (2007) Diffusion-tensor MR imaging and tractography: exploring brain microstructure and connectivity. *Radiology* 245: 367-384.
4. Correia S, Lee SY, Voorn T, Tate DF, Paul RH, et al. (2008) Quantitative tractography metrics of white matter integrity in diffusion-tensor MRI. *Neuroimage* 42: 568-581.
5. Calamante F, Tournier JD, Jackson GD, Connelly A (2010) Track-density imaging (TDI): super-resolution white matter imaging using whole-brain track-density mapping. *Neuroimage* 53: 1233-1243.
6. Calamante F, Tournier JD, Heidemann RM, Anwender A, Jackson GD, et al. (2011) Track density imaging (TDI): validation of super resolution property. *Neuroimage* 56: 1259-1266.
7. Calamante F, Tournier JD, Smith RE, Connelly A (2012) A generalised framework for super-resolution track-weighted imaging. *Neuroimage* 59: 2494-2503.
8. Pannek K, Mathias JL, Bigler ED, Brown G, Taylor JD, et al. (2011) The average pathlength map: a diffusion MRI tractography-derived index for studying brain pathology. *Neuroimage* 55: 133-141.
9. Pannek K, Mathias JL, Rose SE (2011) MRI diffusion indices sampled along streamline trajectories: quantitative tractography mapping. *Brain Connect* 1: 331-338.
10. Ware JB, Biester RC, Whipple E, Robinson KM, Ross RJ, et al. (2016) Combat-related Mild Traumatic Brain Injury: Association between Baseline Diffusion-Tensor Imaging Findings and Long-term Outcomes. *Radiology* 151013.
11. Van Essen DC, Smith SM, Barch DM, Behrens TEJ, Yacoub E, et al. (2013) The WU-Minn Human Connectome Project: An overview. *Neuroimage*.
12. Feinberg DA, Moeller S, Smith SM, Auerbach E, Ramanna S, et al. (2010) Multiplexed Echo Planar Imaging for Sub-Second Whole Brain fMRI and Fast Diffusion Imaging. *PLoS ONE* 5: e15710.
13. Moeller S, Yacoub E, Olman CA, Auerbach E, Strupp J, et al. (2010) Multiband multislice GE-EPI at 7 tesla, with 16-fold acceleration using partial parallel imaging with application to high spatial and temporal whole-brain fMRI. *Magn Reson Med* 63: 1144-1153.
14. Setsompop K, Kimmlingen R, Eberlein E, Witzel T, Cohen-Adad J, et al. (2013) Pushing the limits of in vivo diffusion MRI for the Human Connectome Project. *Neuroimage*.
15. Setsompop K, Gagoski BA, Polimeni JR, Witzel T, Wedeen VJ, et al. (2012) Blipped-controlled aliasing in parallel imaging for simultaneous multislice echo planar imaging with reduced g-factor penalty. *Magn Reson Med* 67: 1210-1224.
16. Behrens TEJ, Johansen-Berg H, Woolrich MW, Smith SM, Wheeler-Kingshott CAM, et al. (2003) Non-invasive mapping of connections between human thalamus and cortex using diffusion imaging. *Nature neuroscience* 6: 750-757.
17. Smith SM, Jenkinson M, Woolrich MW, Beckmann CF, Behrens TEJ, et al. (2004) Advances in functional and structural MR image analysis and implementation as FSL. *Neuroimage* 23: S208-S219.
18. Mori S, Van Zijl PCM (2002) Fiber tracking: principles and strategies- A technical review. *NMR Biomed* 15: 468-480.
19. Smith SM (2002) Fast robust automated brain extraction. *Hum Brain Mapp* 17: 143-155.
20. Klein A, Andersson J, Ardekani BA, Ashburner J, Avants B, et al. (2009) Evaluation of 14 nonlinear deformation algorithms applied to human brain MRI registration. *Neuroimage* 46: 786-802.
21. Rueckert D, Sonoda LI, Hayes C, Hill DL, Leach MO, et al. (1999) Nonrigid registration using free-form deformations: application to breast MR images. *IEEE Trans Med Imaging* 18: 712-721.
22. Smith SM, Jenkinson M, Johansen-Berg H, Rueckert D, Nichols TE, et al. (2006) Tract-based spatial statistics: voxelwise analysis of multi-subject diffusion data. *Neuroimage* 31: 1487-1505.
23. Bazarian JJ, Zhu T, Blyth B, Borrino A, Zhong J (2012) Subject-specific changes in brain white matter on diffusion tensor imaging after sports-related concussion. *Magn Reson Imaging* 30: 171-180.

24. Mac Donald CL, Johnson AM, Cooper D, Nelson EC, Werner NJ, et al. (2011) Detection of Blast-Related Traumatic Brain Injury in U.S. Military Personnel. *New Eng J Med* 364: 2091-2100.
25. Watts R, Thomas A, Filippi CG, Nickerson JP, Freeman K (2014) Potholes and Molehills: Bias in the Diagnostic Performance of Diffusion-Tensor Imaging in Concussion. *Radiology* 31856.
26. Rashid W, Hadjiprocopis A, Griffin CM, Chard DT, Davies GR, et al. (2004) Diffusion tensor imaging of early relapsing-remitting multiple sclerosis with histogram analysis using automated segmentation and brain volume correction. *Mult. Scler* 10: 9-15.
27. Roalf DR, Ruparel K, Verma R, Elliott MA, Gur RE, et al. (2013) White matter organization and neurocognitive performance variability in schizophrenia. *Schizophr* 143: 172-178.
28. Shimony JS, McKinstry RC, Akbudak E, Aronovitz JA, Snyder AZ, et al. (1999) Quantitative diffusion-tensor anisotropy brain MR imaging: normative human data and anatomic analysis. *Radiology* 212: 770-784.
29. Mori S, Frederiksen K, van Zijl PCM, Stieltjes B, Kraut MA, et al. (2002) Brain white matter anatomy of tumor patients evaluated with diffusion tensor imaging. *Ann Neurol* 51: 377-380.
30. Cauley KA, Burbank HN, Filippi CG (2009) Diffusion tensor imaging and tractography of Rasmussen encephalitis. *Pediatr Radiol* 39: 727-730.
31. Klöppel S, Draganski B, Golding CV, Chu C, Nagy Z, et al. (2008) White matter connections reflect changes in voluntary-guided saccades in pre-symptomatic Huntington's disease," *Brain* 131: 196-204.
32. Nucifora PG, Kim J (2014) Processing speed and connectivity in traumatic brain injury. Annual Meeting of the American Society for Functional Neuroradiology, Miami.
33. Field AS, Alexander AL, Wu YC, Hasan KM, Witwer B, et al. (2004) Diffusion tensor eigenvector directional color imaging patterns in the evaluation of cerebral white matter tracts altered by tumor. *J Magn Reson Imaging* 20: 555-562.
34. Jones DK, Knösche TR, Turner R (2012) White matter integrity, fiber count, and other fallacies: The do's and don'ts of diffusion MRI. *NeuroImage*.
35. Behrens TEJ, Woolrich MW, Jenkinson M, Johansen-Berg H, Nunes RG, et al. (2003) Characterization and propagation of uncertainty in diffusion-weighted MR imaging," *Magn Reson Med* 50: 1077-1088.